SUPPLEMENTARY FIGURES AND TABLES LEGEND

Supplementary Figure 1. Locations where each aerosol sample was collected during Leg 1 (Malta to Kuwait).

Supplementary Figure 2. Locations where each aerosol sample was collected during Leg 2 (Kuwait to Toulon).

Supplementary Figure 3. Time series of dust concentrations estimated from the Ca+ concentrations measured in the water-soluble fraction of total suspended particles. Red markers show where hourly composition data was linearly interpolated for four samples where data was partially missing (samples f020, f025, f036 and f037).

Supplementary Figure 4. Aerosol sampling set-up on the RV *Kommandor Iona* wheelhouse top.

Supplementary Figure 5. INP concentrations measured in 8 aerosol samples from which a dilution was performed (10-100X). The n_{INP} spectra from both the original suspension and the dilution are shown (see Methods Sec 2.4).

Supplementary Figure 6. INP concentrations measured in 26 aerosol samples collected during AQABA and in simulated INP concentrations from 7 blank filter samples. The simulated blank filter INP concentrations were estimated for the mean volume sampled during AQABA (6680 L, see Methods Sec 2.4). The freezing onset temperatures detected in 6 of the 7 field blanks ranged between -15 and -27 °C, with the exception of one field blank sample in which a single freezing event was detected at a relatively higher temperature -6 °C. This indicates the presence of a rare contaminant with a high freezing temperature from sampling handling processes, as this single freezing event represented 1/255 of total detected field blank freezing events. The INP concentrations measured in one aerosol sample (f033) fell within the range of background INP levels present in field blanks.

Supplementary Figure 7. Linear regressions between total aerosol surface area and concentrations of INPs with freezing temperatures between -10 and -20 °C. Results show little to no correlation between INP concentrations and total aerosol surface area. R^2 and *p* values are also reported for each temperature. Shaded region is the 95% confidence interval for the best fit linear regression. Marker colors indicate the average ambient dust mass concentration during the sampling period. Dilutions of 8 filter samples are included in the regression analysis (Fig. S5).

Supplementary Figure 8. Aerosol 72-hour back trajectories for Leg 1 simulated by FLEXPART (Methods Sec. 2.5).

Supplementary Figure 9. Aerosol 72-hour back trajectories for Leg 2 simulated by FLEXPART (Methods Sec. 2.5). Sample f033 marked with an X to indicate no INPs detected at -15 °C.

Supplementary Figure 10. Map of the collection locations of 10 subsurface seawater (SSW) samples. Marker sizes indicate abundance of INPs.

Supplementary Figure 11. Average ocean surface chlorophyll *a* concentration from 1 August to 31 August 2017 (Moderate Resolution Imaging Spectroradiometre, https://oceandata.sci.gsfc.nasa.gov/MODIS-Aqua).

Supplementary Figure 12. Measured concentrations of INPs in SSW samples that were treated with heat, hydrogen peroxide and a 0.2 μm filter (Methods Sec. 2.4). Results indicate the presence of organic, heat-labile and heat-stable INPs, and an abundance of INPs both larger and smaller than 0.2 μm.

Figure S1

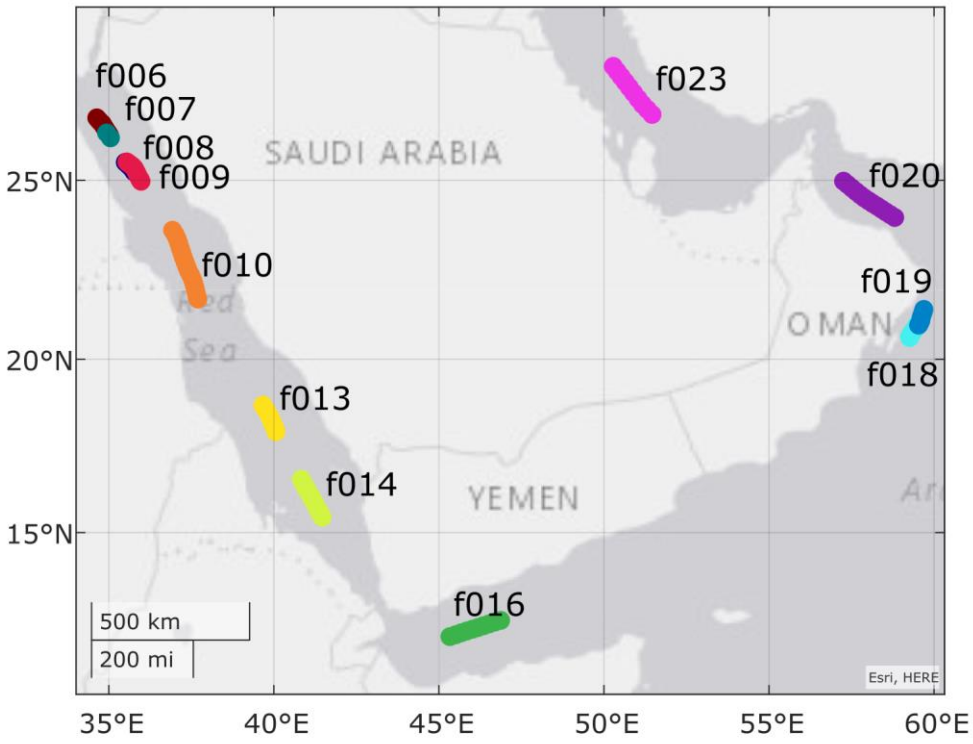
f006
f007
f008
f009
f010
f013
f014
f016
f023
f020
f019
f018
SAUDI ARABIA
YEMEN
O MAN
Red
Sea
25°N
20°N
15°N
35°E
40°E
45°E
50°E
55°E
60°E
500 km
200 mi
Esri, HERE

Figure S2

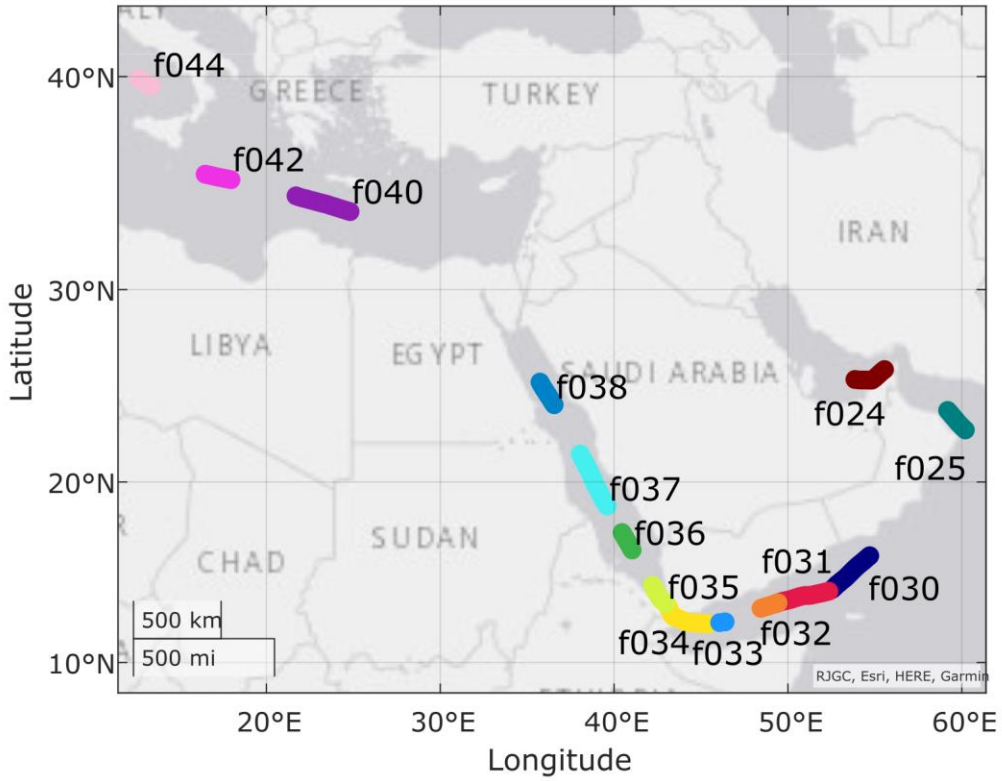
f044
f042
f040
f038
f024
f025
f037
f036
f031
f030
f035
f034
f033
f032
GREECE
TURKEY
IRAN
LIBYA
EGYPT
SAUDI ARABIA
SUDAN
CHAD
500 km
500 mi
RJGC, Esri, HERE, Garmin
40°N
30°N
20°N
10°N
20°E
30°E
40°E
50°E
60°E
Latitude
Longitude

Figure S3

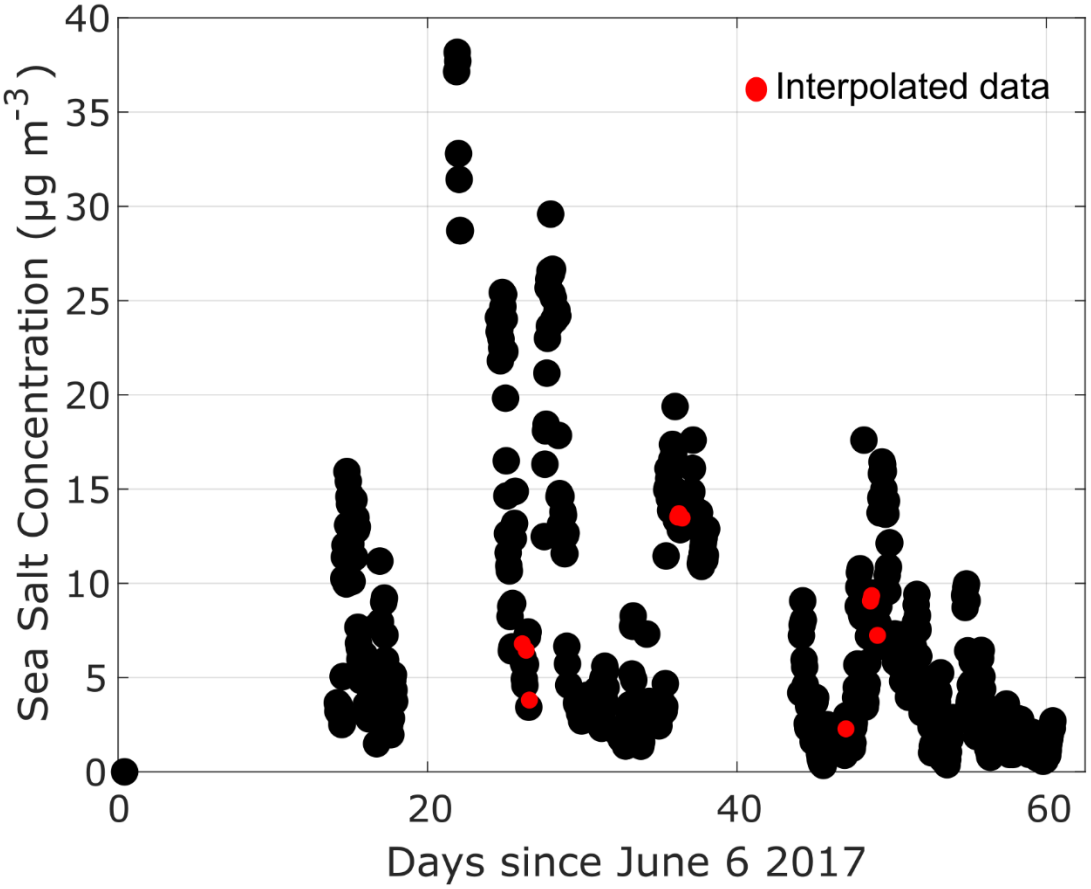
Interpolated data
Sea Salt Concentration (µg m-3)
Days since June 6 2017
0
5
10
15
20
25
30
35
40
0
20
40
60

Figure S4

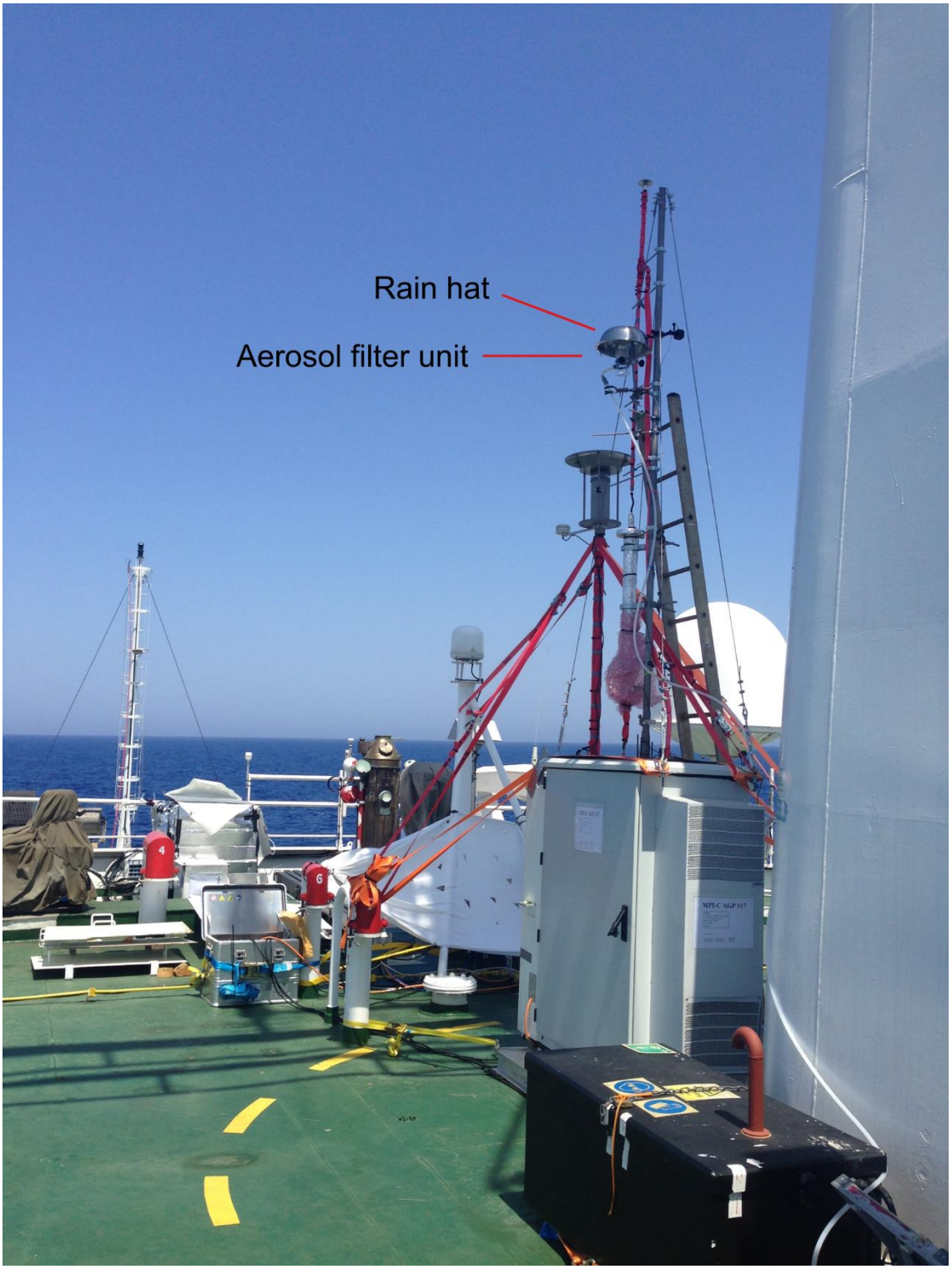

Figure S5

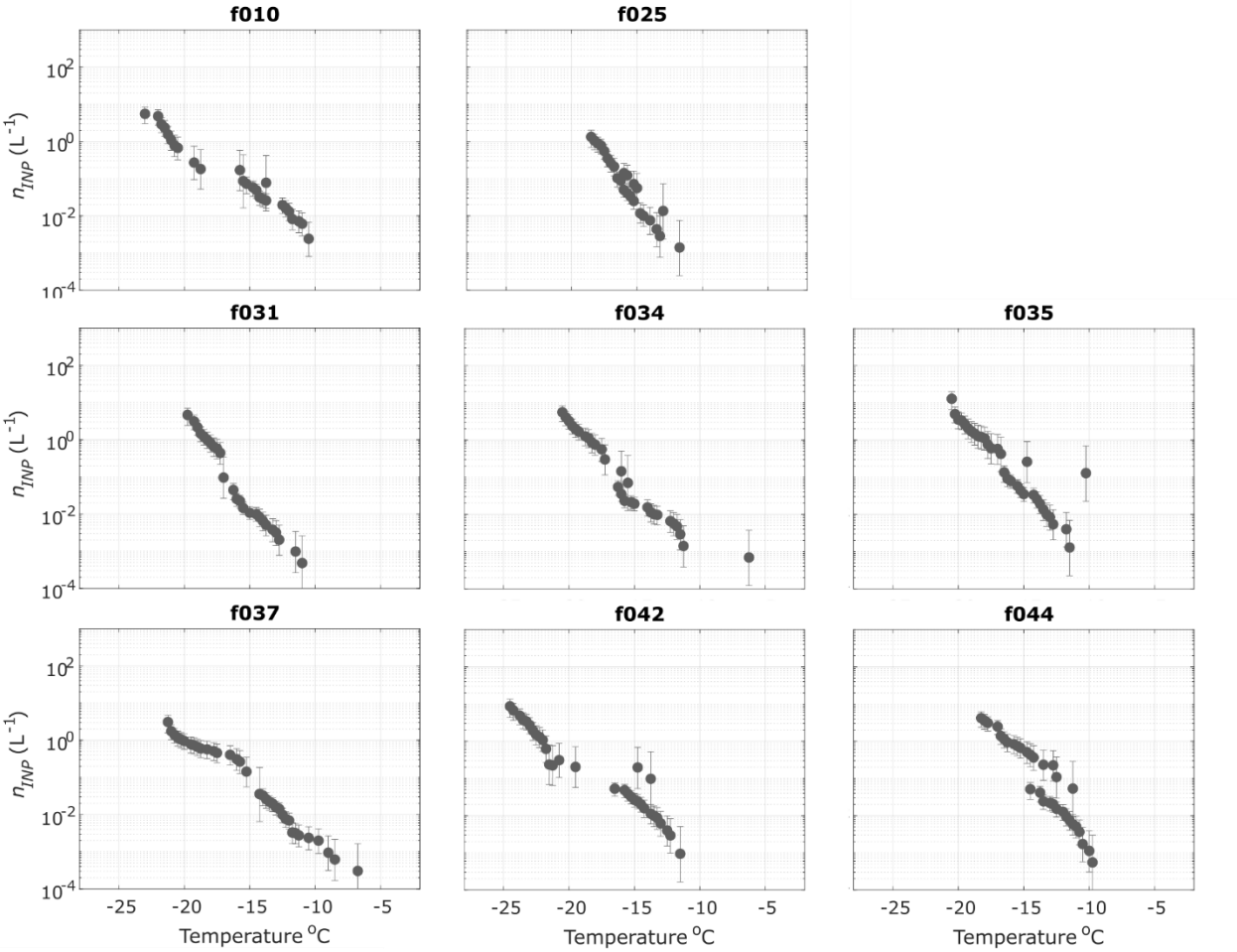
f010
f025
f031
f034
f035
f037
f042
f044
n_{INP} (L^{-1})
10^{2}
10^{0}
10^{-2}
10^{-4}
-25
-20
-15
-10
-5
Temperature ^{o}C

Figure S6

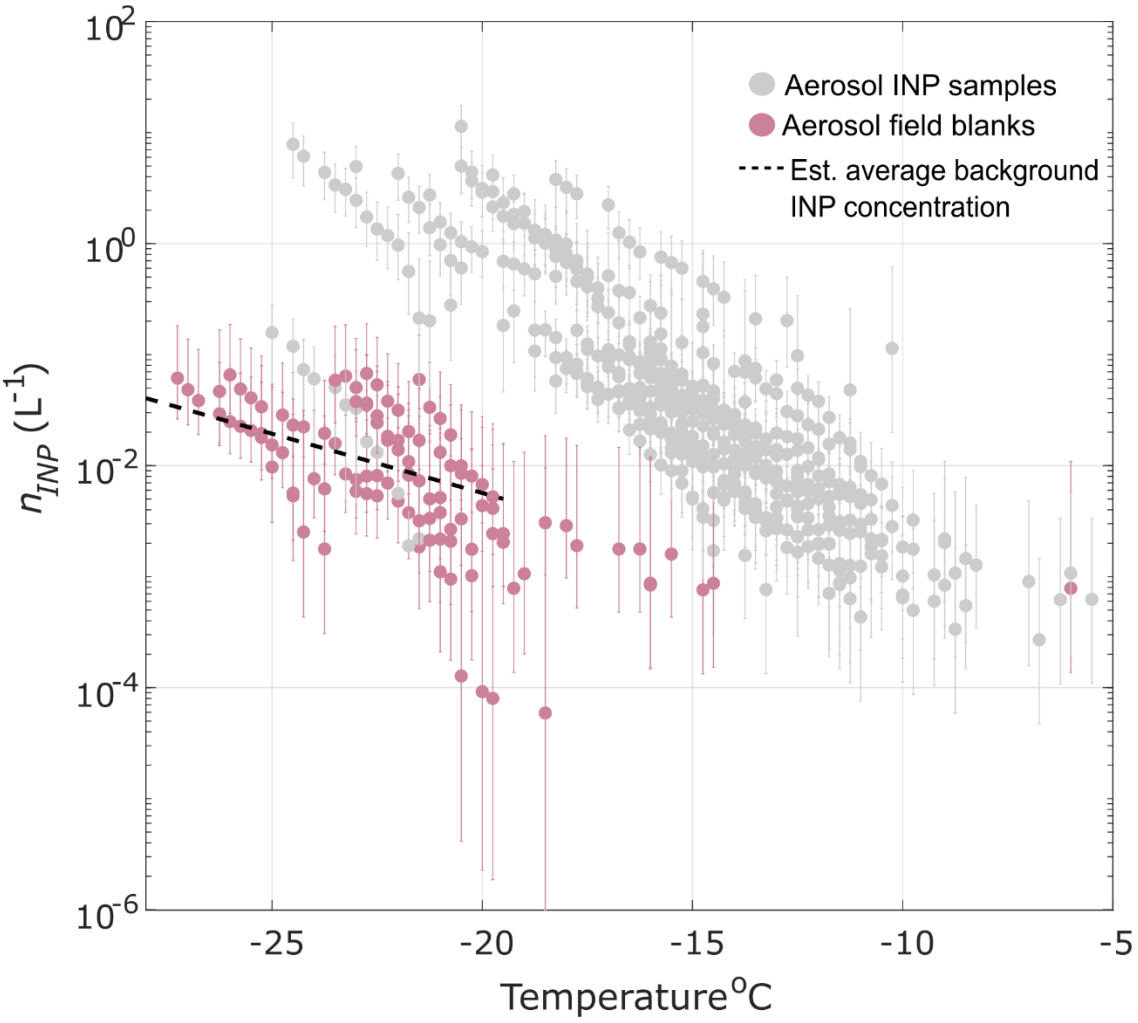
Aerosol INP samples
Aerosol field blanks
Est. average background INP concentration
n_{INP} (L^{-1})
10^{2}
10^{0}
10^{-2}
10^{-4}
10^{-6}
-25
-20
-15
-10
-5
Temperature°C

Figure S7

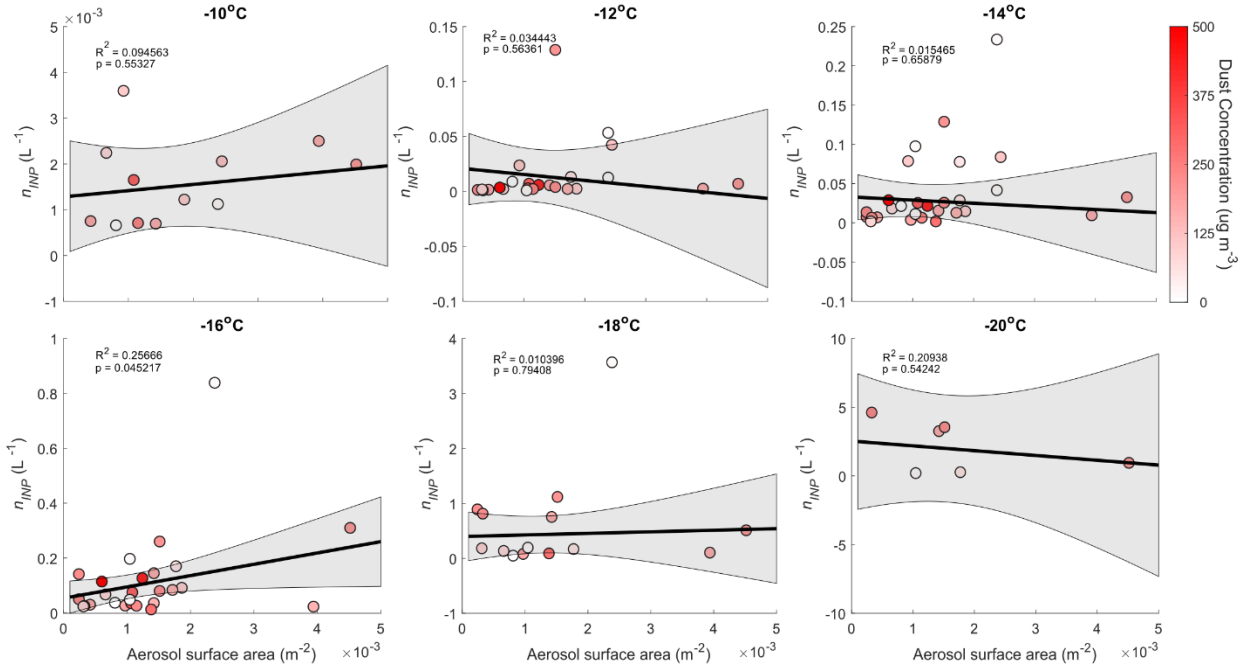
-10°C
R² = 0.094563
p = 0.55327
-12°C
R² = 0.034443
p = 0.56361
-14°C
R² = 0.015465
p = 0.65879
-16°C
R² = 0.25666
p = 0.045217
-18°C
R² = 0.010396
p = 0.79408
-20°C
R² = 0.20938
p = 0.54242
n_INP (L⁻¹)
Aerosol surface area (m⁻²)
×10⁻³
Dust Concentration (ug m⁻³)

Figure S8

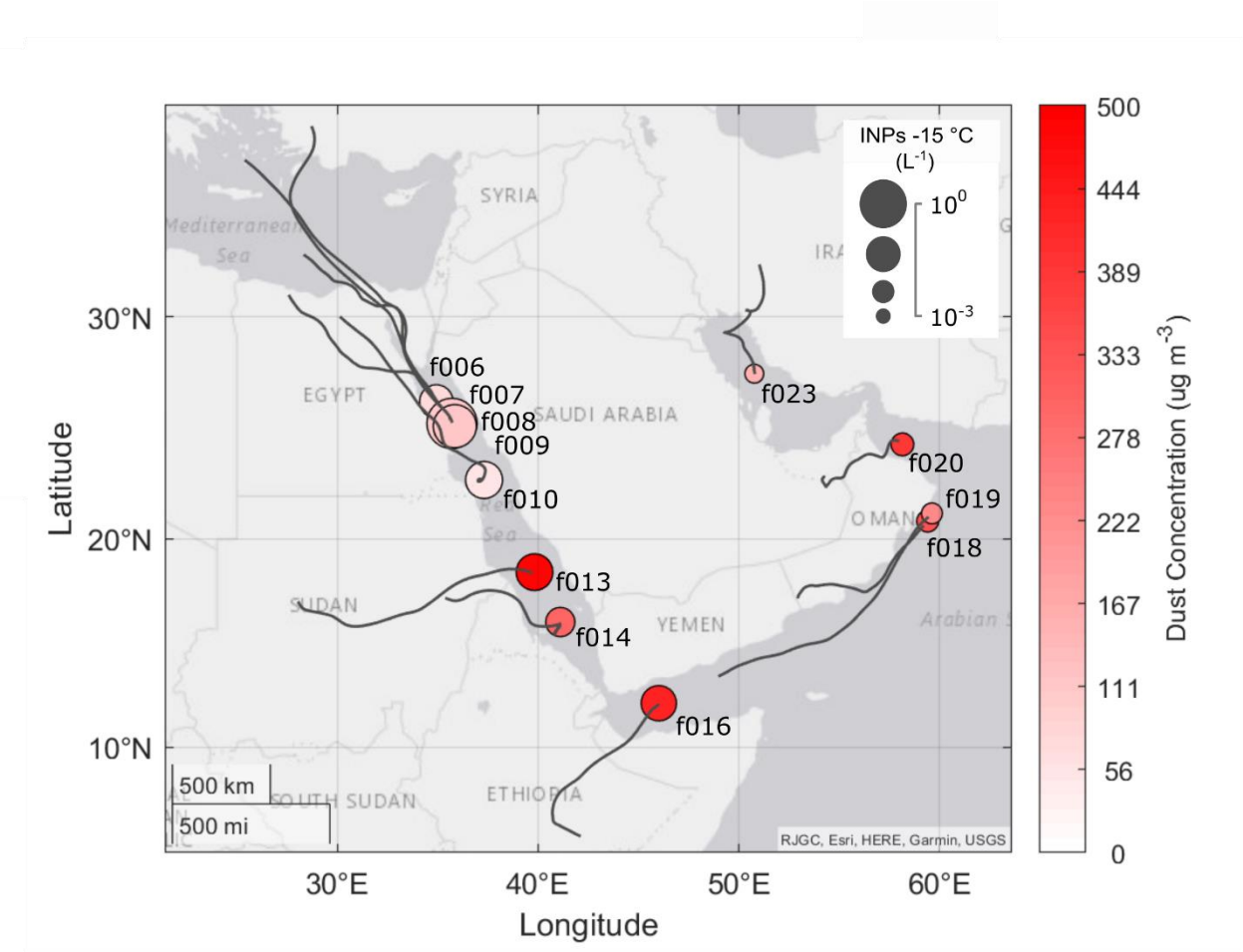
INPs -15 °C
(L-1)
10^0
10^-3
SYRIA
EGYPT
SAUDI ARABIA
SUDAN
YEMEN
OMAN
ETHIOPIA
SOUTH SUDAN
Mediterranean Sea
Red Sea
Arabian S
f006
f007
f008
f009
f010
f013
f014
f016
f018
f019
f020
f023
500 km
500 mi
RJGC, Esri, HERE, Garmin, USGS
30°N
20°N
10°N
30°E
40°E
50°E
60°E
Latitude
Longitude
500
444
389
333
278
222
167
111
56
0
Dust Concentration (ug m-3)

Figure S9

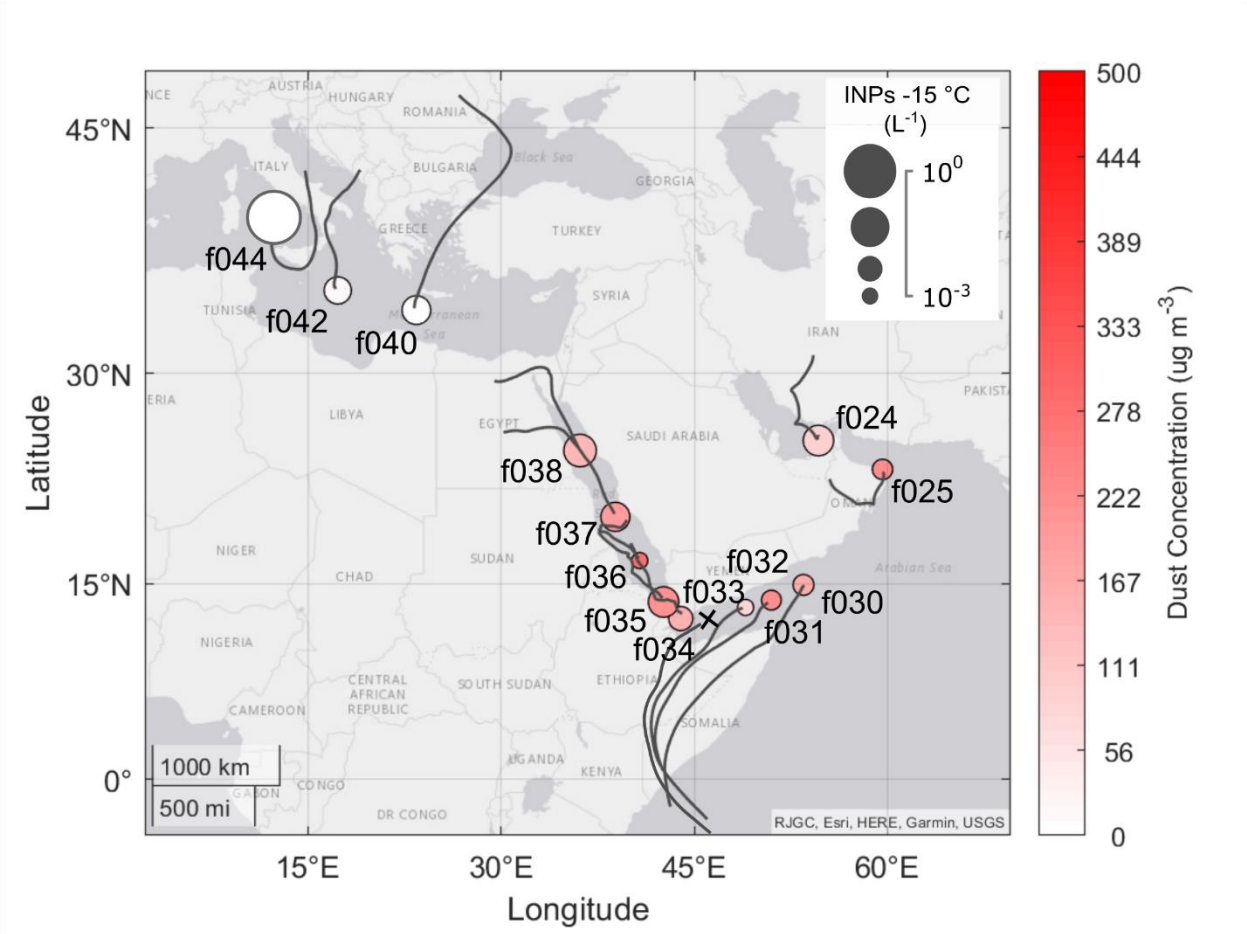
INPs -15 °C
(L-1)
10^0
10^-3
f044
f042
f040
f038
f037
f036
f035
f034
f033
f032
f031
f030
f025
f024
45°N
30°N
15°N
0°
15°E
30°E
45°E
60°E
Latitude
Longitude
1000 km
500 mi
RJGC, Esri, HERE, Garmin, USGS
Dust Concentration (ug m-3)
500
444
389
333
278
222
167
111
56
0
AUSTRIA
HUNGARY
ROMANIA
ITALY
BULGARIA
GREECE
TURKEY
SYRIA
IRAN
TUNISIA
LIBYA
EGYPT
SAUDI ARABIA
NIGER
CHAD
SUDAN
NIGERIA
CAMEROON
CENTRAL AFRICAN REPUBLIC
SOUTH SUDAN
ETHIOPIA
SOMALIA
UGANDA
KENYA
CONGO
DR CONGO
GEORGIA
Black Sea
Arabian Sea

Figure S10

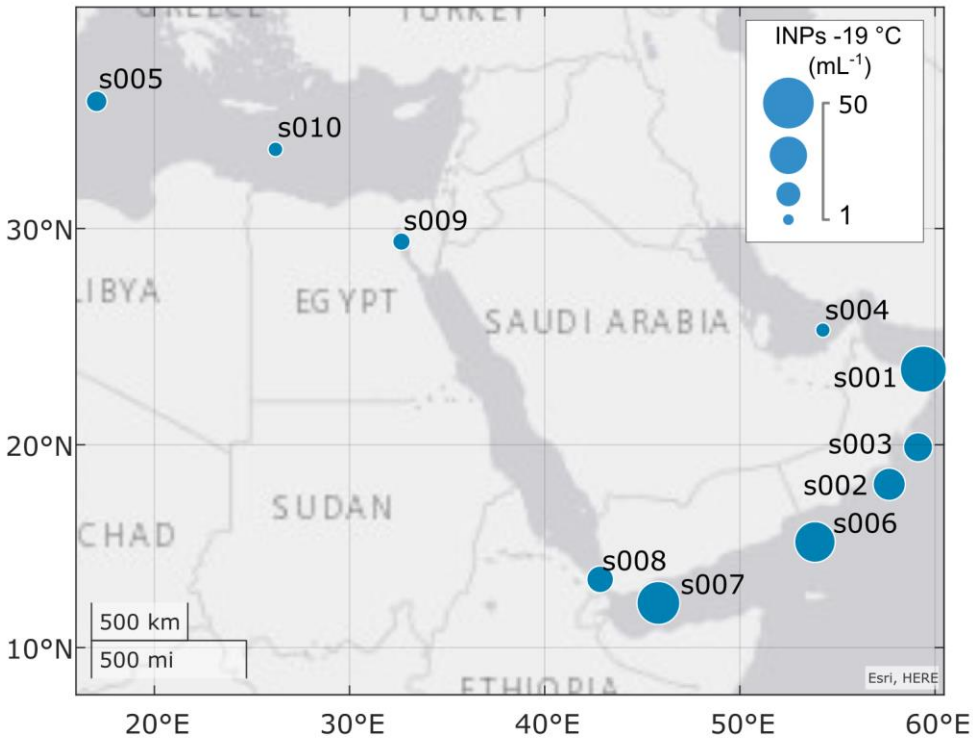
INPs -19 °C
(mL-1)
50
1
s005
s010
s009
s004
s001
s003
s002
s006
s008
s007
LIBYA
EGYPT
SAUDI ARABIA
SUDAN
CHAD
ETHIOPIA
500 km
500 mi
Esri, HERE
30°N
20°N
10°N
20°E
30°E
40°E
50°E
60°E

Figure S11

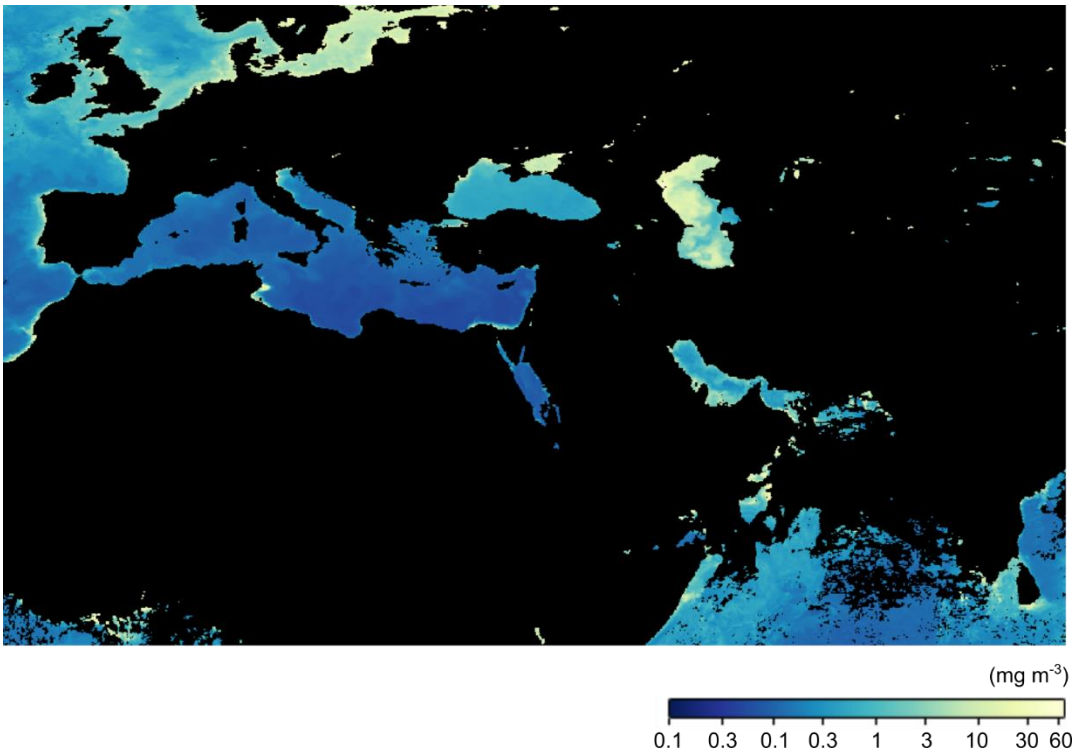

Figure S12

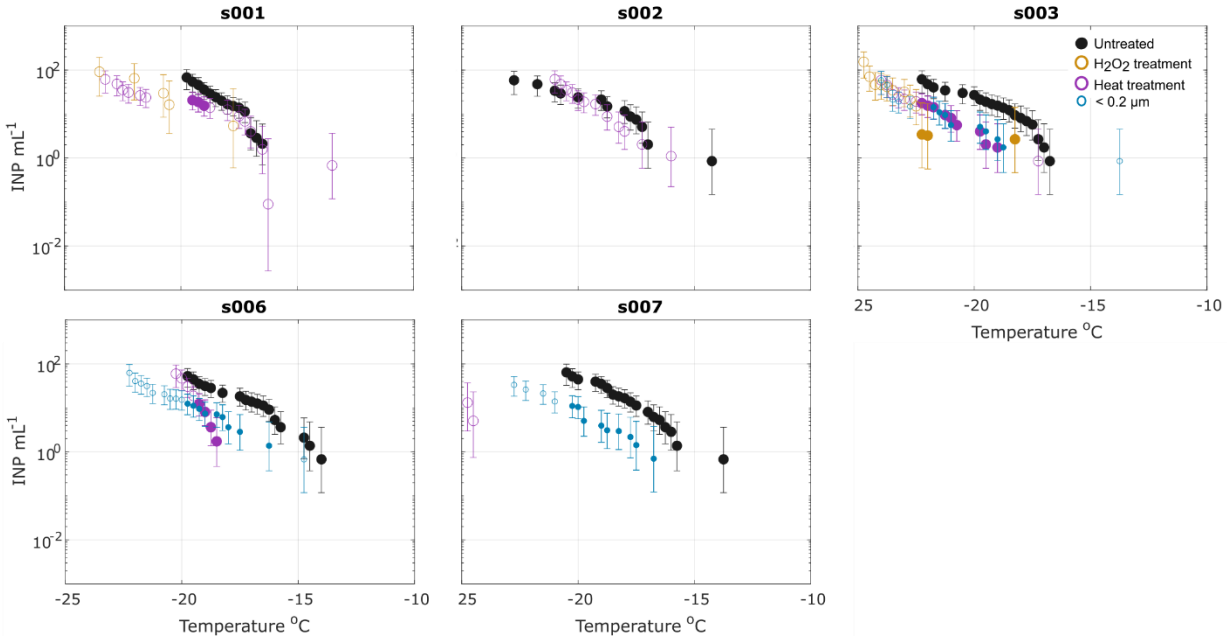
s001
s002
s003
s006
s007
INP mL-1
Temperature °C
Untreated
H2O2 treatment
Heat treatment
< 0.2 µm